Eur. Phys. J. B (2021)94:116
https://doi.org/10.1140/epjb/s10051-021-00130-x

THE EUROPEAN PHYSICAL JOURNAL B

Regular Article - Solid State and Materials

Superfluid density and critical current density in superconducting cuprates with an extended d-wave pairing symmetry

Orifjon K. Ganiev[1,2,a] and Bakhrom Ya. Yavidov[3]

[1] Institute of Nuclear Physics, Uzbekistan Academy of Sciences, 100214 Tashkent, Uzbekistan
[2] Faculty of Physics, National University of Uzbekistan, 100174 Tashkent, Uzbekistan
[3] Nukus State Pedagogical Institute named after A'jiniyaz, 230105 Nukus, Uzbekistan

Received 4 April 2021 / Accepted 15 May 2021

Abstract. In this paper, we have investigated superfluid density, ρ_s, and the critical current density, J_c, in cuprate superconductors. The Chandrasekhar and Einzel approach was applied to calculate the superconducting order parameter and superfluid density with different pairing scenario, such as isotropic s-, anisotropic s-wave, and nodal d-wave, as well as an extended d-wave symmetry of the gap. Moreover, the critical current density is calculated for the extended d-wave gap suggested by angle-resolved photoemission spectroscopy (ARPES) mesurements in anisotropic cuprate superconductors. The calculated results for the temperature-dependent superfluid density $\rho_s(T)$ and critical current density $J_c(T)$ were compared with the experimental data obtained for various cuprate superconductors. A good quantitative agreement was found between theory and experimental data for all cases considered.

1 Introduction

Among many superconducting properties, the symmetry of the order parameter is an important one. It is usually assumed that the order parameter in high-temperature superconducting cuprates (HTSCs) has a pure d-wave symmetry. Corresponding evidence of this assumption for both the electron- and the hole-doped classes of HTSCs stems from experiments where mainly surface phenomena are probed. In this regard, angle-resolved photoemission spectroscopy (ARPES) mesurements in anisotropic cuprate superconductors have given key information on the temperature and angle dependence of the superconducting energy gap. The early suggestion is that superconductivity in cuprate superconductors might exhibit unconventional d-wave symmetry of the order parameter [1–3]. For hole-doped cuprate superconductors, it has been well documented that the superconducting energy gap has a d-wave form $\Delta = \Delta_0 \cos(2\varphi)$. This basic form of the d-wave superconducting energy gap was first observed in ARPES experiments [4,5]. While the symmetry of the superconducting energy gap is believed to be d-wave for the hole-doped region, the situation for electron-doped superconducting materials is more controversial.

Recently, Khasanov et al. [6] obtained the temperature dependencies of the in-plane (λ_{ab}) and out-of-plane (λ_c) components of the magnetic field penetration depth of the electron-doped superconductor $Sr_{0.9}La_{0.1}CuO_2$ using magnetization measurements. The measured λ_{ab} and λ_c have analyzed in terms of a two-gap model with mixed $s+d$-wave symmetry of the order parameter. Furthermore, several studies [7–9,11] have suggested that the angular dependence of the gap function in electron-doped cuprates can significantly differ from the simple functional form $\Delta_0 \cos(2\varphi)$, which appears to describe hole-doped cuprates.

Especially, the superconducting energy gap is significantly nonlinear in the vicinity of the nodal directions. In this regard, evaluation and analysis of the temperature-dependent superfluid density in superconductors is a powerful tool for studying pairing symmetry [12,13]. Although it does not detect order parameter phase, this bulk probe is very sensitive to the gap structure on the Fermi surface. Therefore it can be used to verify the conclusions provided by the gap-mapping techniques such as ARPES [14–19] or directional tunneling using scanning tunneling spectroscopy (STS) [20–23]. The ARPES investigations produce a direct and high resolution measurements of the normal and quasiparticle density of states around the Fermi surface in superconductors. It is mainly motivated by the search for reliable data in the study of unconventional superconductors, including cuprates. Also, ARPES experiments suggest that the gap variation on the Fermi surface in HTSC should take into account long-range electron-phonon interactions, which leads to the inclusion of the higher angle harmonics, consistent with the

[a] e-mail: orif.ganiev@gmail.com (corresponding author)

Published online: 28 May 2021

d-wave symmetry of the gap. In addition, from the point of view of the possibility of any large-scale practical application of superconductivity, it depends primarily on the maximum current density that superconductors can carry in one way or another.

In the present paper, we examine the impact of pairing symmetry on the superconducting gap, superfluid density and critical current density in cuprate superconductors. In this regard, using the Chandrasekhar and Einzel approach, we calculate the superfluid density from the temperature dependence of the superconducting energy gap $\Delta(T)$, thus allowing us to fit critical current density data for cuprate superconductors.

2 Typical gap functions for singlet pairing states

The microscopic superconducting state formed as a result of condensation of the Cooper pairs is protected by the energy gap. The pairing interaction between the two electron of a Cooper pair determines the superconducting energy gap function. Thus, it is important to determine the structure of the gap in order to understand the mechanism of superconductivity. In high-T_c cuprate superconductors, it has been well established that the superconducting energy gap may have a d-wave function.

The importance of the superconducting energy gap function becomes apparent at nonzero temperatures, when it is possible to generate quasiparticle excitations and a paramagnetic current. In order to use Chandrasekhar and Einzel model for calculating superfluid density, a form for the gap function is required. For spin singlet pairing states takes the form,

$$\Delta(T,\mathbf{k}) = \Delta_0(T)g(\mathbf{k}) \tag{1}$$

where $g(\mathbf{k})$ is the dimensionless function of maximum unit magnitude that describes the angular variation of the superconducting energy gap on the Fermi surface. $\Delta_0(T)$ carries the temperature dependence and should be determined from the self-consistent gap equation. The latter involves a Fermi surface average of $g(\mathbf{k})$, so in general $\Delta_0(T)$ depends on the pairing symmetry.

An extended d-wave gap function can be written as [25]

$$\begin{aligned}\Delta(T,\varphi) &= \Delta_0(T)g(\varphi)\\ &= \Delta_0(T)[B\cos(2\varphi) + (1-B)\cos(6\varphi)]\end{aligned} \tag{2}$$

where B is the doping-dependent fitting parameter, $\cos(6\varphi)$ denotes the next harmonic corresponding to the d-wave symmetry of the gap.

In addition, the anisotropic s-wave gap function with two- and four-fold symmetry has the following form, respectively [9,10]

$$\Delta(T,\varphi) = \Delta_0(T)|[\cos(2\varphi) - A\cos(6\varphi)]|, \tag{3}$$

and

$$\Delta(T,\varphi) = \Delta_0(T)[1 + A\cos(4\varphi)], \tag{4}$$

where the parameter A defines an anisotropy.

3 The superfluid density for different superconducting pairing symmetries

In this section, we will briefly describe the main results of a semi-classical approach for the penetration depth proposed by Chandrasekhar and Einzel [24]. Taking into account a Fermi surface and the gap function, this approach provides a generalized relationship between the supercurrent response to the magnetic vector potential given an arbitrary band structure and energy gap. We restrict ourselves to singlet pairing states.

In an anisotropic superconductor and in the London approximation ($\lambda > \xi$), the supercurrent density $\mathbf{J}$ is related to the vector potential $\mathbf{A}$ by a response tensor $\mathbb{T}$ so that

$$\mathbf{J} = -\mathbb{T}\mathbf{A}, \tag{5}$$

and the response tensor can be defined as follows

$$\mathbb{T} = \frac{e^2}{4\pi^3 c}\int \mathrm{d}^3k\left(-\frac{\partial n_k}{\partial \varepsilon_k} + \frac{\partial f(E_k)}{\partial E_k}\right)(\mathbf{v}_k\mathbf{v}_k). \tag{6}$$

The penetration depth components along a specific direction with respect to the crystalline axes can be computed by using the relationship

$$\lambda_{ii} = \left(\frac{c}{4\pi T_{ii}}\right)^{1/2}, \quad i = x,y,z \tag{7}$$

and it should be noted that the λ_{ii} are not the components of a vector or a tensor, but rather are the different penetration depths with respect to the crystalline axes. However, the effective mass can be defined by

$$m_{ii} = \frac{ne^2}{cT_{ii}}, \tag{8}$$

which gives us the familiar London relation

$$\lambda_{ii} = \left(\frac{m_{ii}c^2}{4\pi^2}\right)^{1/2}. \tag{9}$$

Consider now the structure of the response tensor, $\mathbb{T}$, shown in Eq. (6). The response tensor consists of two terms which usually are called the diamagnetic and the paramagnetic terms ($\mathbb{T}_\mathrm{D}$) and ($\mathbb{T}_\mathrm{P}$), such that

$$\mathbb{T} = \mathbb{T}_\mathrm{D} - \mathbb{T}_\mathrm{P}. \tag{10}$$

The above two terms of the response tensor are related to the normal and superconducting state properties according to the formulas

$$\mathbb{T}_{\mathrm{D}} = \frac{e^2}{4\pi^3 c}\int \mathrm{d}^3k \left(-\frac{\partial n_k}{\partial \varepsilon_k}\right)(\mathbf{v}_k\mathbf{v}_k) \tag{11}$$

and

$$\mathbb{T}_{\mathrm{P}} = \frac{e^2}{4\pi^3 c}\int \mathrm{d}^3k \left(-\frac{\partial f(E_k)}{\partial E_k}\right)(\mathbf{v}_k\mathbf{v}_k) \tag{12}$$

By considering the fact that the derivatives in Eqs. (11) and (12) are zero unless $|\varepsilon_k - \mu| \lesssim \Delta(k)$ and also that $\Delta(k) << \mu$, the value of the tensor $\mathbf{v}_k\mathbf{v}_k$ can be replaced by its value at $\varepsilon_k = \mu$, which is $\mathbf{v}_{\mathrm{F}}\mathbf{v}_{\mathrm{F}}$. For this same reason, we can make the substitution

$$\mathrm{d}^3k \longrightarrow \frac{\mathrm{d}S_{\mathrm{F}}\mathrm{d}\varepsilon_k}{\hbar|\mathbf{v}_k|} \tag{13}$$

where $\mathrm{d}S_{\mathrm{F}}$ is a constant energy surface element and $\mathbf{v}_k$ is the magnitude of the Fermi velocity. These approximations give us

$$\begin{aligned}\mathbb{T}_{\mathrm{D}} &= \frac{e^2}{4\pi^3\hbar c}\oint \mathrm{d}S_{\mathrm{F}}\int_0^\infty \mathrm{d}\varepsilon_k\left(-\frac{\partial n_k}{\partial\varepsilon_k}\right)\frac{\mathbf{v}_k\mathbf{v}_k}{|\mathbf{v}_{\mathrm{F}}|}\\ &\cong \frac{e^2}{4\pi^3\hbar c}\oint \mathrm{d}S_{\mathrm{F}}\frac{\mathbf{v}_k\mathbf{v}_k}{|\mathbf{v}_{\mathrm{F}}|}\end{aligned} \tag{14}$$

and

$$\begin{aligned}\mathbb{T}_{\mathrm{P}} \cong 2\cdot\frac{e^2}{4\pi^3\hbar c}\oint \mathrm{d}S_{\mathrm{F}}\frac{\mathbf{v}_k\mathbf{v}_k}{|\mathbf{v}_{\mathrm{F}}|}\\ \times\int_{\Delta(k)}^\infty dE_k\left(-\frac{\partial f(E_k)}{\partial E_k}\right)\frac{E_k}{\sqrt{E_k^2-\Delta^2(k)}}.\end{aligned} \tag{15}$$

where $f(E_k) = (e^{E_k/k_BT}+1)^{-1}$ is the Fermi-Dirac distribution function, k_B is Boltzmann's constant.

It should be noted that the analysis of Eqs. (14) and (15) leads to the following conclusions:

(i) As $T \longrightarrow 0$, $\mathbb{T}_{\mathrm{P}} \longrightarrow 0$ and as $T \longrightarrow T_{\mathrm{c}}$, $\mathbb{T}_{\mathrm{P}} \longrightarrow \mathbb{T}_{\mathrm{D}}$.
(ii) If $\Delta(k)$ is anisotropy of $\mathbb{T}_{\mathrm{P}}$ is temperature-independent and its anisotropy is the same as the anisotropy of $\mathbb{T}_{\mathrm{D}}$.
(iii) If $\Delta(k)$ is anisotropic, then the anisotropy of $\mathbb{T}_{\mathrm{P}}$ is affected by the anisotropies of both ε_k and $\Delta(k)$, and is temperature-dependent.

The normalized superfluid density, $\rho_{\mathrm{s}}(T)$, is the ratio of the concentration of superconducting electrons to the total concentration of available charge and can be related to the penetration depth by

$$\rho_{\mathrm{s}}(T) = \frac{n_{\mathrm{s}}(T)}{n_{\mathrm{s}}(0)} = \left(\frac{\lambda(0)}{\lambda(T)}\right)^2 \tag{16}$$

Then the normalized superfluid density components can be calculated as

$$\rho_{ii} = \frac{\lambda_{ii}^2(0)}{\lambda_{ii}^2(T)} = \frac{\mathbb{T}_{ii}(T)}{\mathbb{T}_{ii}(0)}, \tag{17}$$

where generally we have

$$\begin{aligned}\mathbb{T}_{ij} = \frac{e^2}{4\pi^3\hbar c}\oint_{FS}\mathrm{d}S_{\mathrm{F}}\\ \times\left[\frac{\mathrm{v}_{\mathrm{F}}^i\mathrm{v}_{\mathrm{F}}^j}{|\mathbf{v}_{\mathrm{F}}|}\left(1+2\int_{\Delta(k)}^\infty\frac{\partial f(E)}{\partial E}\frac{N(E)}{N(0)}\mathrm{d}E\right)\right]\end{aligned} \tag{18}$$

where $N(E)$ is the quasiparticle density of states and $E = \sqrt{\varepsilon_k^2 - \Delta^2(k)}$ is the quasiparticle energy spectrum.

By using Eqs. (17) and (18), the superfluid density can be calculated in terms of the superconducting gap,Δ, and the single particle excitation energy with respect to the Fermi level, ε_{F}, in a straightforward way for a general Fermi surface geometry. Equation (18) provides the connection between the experimentally measured penetration depth and the microscopic superconducting state.

Expressions for the normalized superfluid density can be obtained for two general cases of pairing symmetry. For isotropic s-wave pairing of both two-dimensional (2D) cylindrical and three-dimensional (3D) spherical Fermi surfaces, the integral can be simplified by giving the normalized superfluid density as [12],

$$\begin{aligned}\rho_{\mathrm{s}}(T) = \left(\frac{\lambda(0)}{\lambda(T)}\right)^2 = 1 - \frac{1}{2\pi k_BT}\\ \times\int_0^\infty\cosh^{-2}\left(\frac{\sqrt{\varepsilon^2+\Delta^2(T)}}{2k_BT}\right)\mathrm{d}\varepsilon.\end{aligned} \tag{19}$$

Also for d-wave cuprate superconductors with a 2D cylindrical Fermi surface, the temperature dependence of the normalized superfluid density can be simplified in the form

$$\begin{aligned}\rho_{\mathrm{s}}(T) = 1 - \frac{1}{2\pi k_BT}\int_0^{2\pi}\begin{pmatrix}\cos^2(\varphi)\\ \sin^2(\varphi)\end{pmatrix}\\ \times\int_0^\infty\cosh^{-2}\left(\frac{\sqrt{\varepsilon^2+\Delta^2(T,\varphi)}}{2k_BT}\right)\mathrm{d}\varepsilon\mathrm{d}\varphi.\end{aligned} \tag{20}$$

where φ is the angle around the Fermi surface subtended at (π, π) in the Brillouin zone and $\Delta(\varphi)$ is the angular dependence of the superconducting energy gap function due to the variation of the gap around the Fermi surface.

To calculate the superfluid density, the temperature dependence of the gap magnitude has to be determined from the self-consistent gap equation. The self-consistent equation of the gap depends on the pairing symmetry and the details of the Fermi surface, it takes the form

$$\int_0^{2\pi}\int_0^{\infty} g(\varphi)^2 \left[\frac{\tanh\left[\frac{1}{2k_BT}\sqrt{\varepsilon^2+[\Delta(T)g(\varphi)]^2}\right]}{\sqrt{\varepsilon^2+[\Delta(T)g(\varphi)]^2}} - \frac{1}{\varepsilon}\tanh\frac{\varepsilon}{2}\right] \mathrm{d}\varepsilon \mathrm{d}\varphi = 0. \tag{21}$$

Upon calculating superconducting energy gap from Eq. (21), and then, in turn superfluid density from Eq. (20) one will be able to calculate the critical current density. So that the critical current density can be written as follows:

$$J_c(T) = 2e\rho_s(T)v_c(T), \tag{22}$$

with critical velocity of superfluid carriers,

$$v_c(T) = \sqrt{\frac{\Delta(T,\varphi)}{m_c}}, \tag{23}$$

where m_c is the effective mass of charge carrier.

4 Numerical results and discussion

The pairing state of high-T_c superconductors has not been fully understood, though many experimental results supporting the d-wave pairing have been reported. In addition, it follows from many experimental and theoretical studies that in order to study the influence of order parameters on the behavior of the superfluid density and critical current density, it is important to know the pairing symmetry. Now we will show the influence of the different order parameter symmetries to the temperature-dependent curves of the superfluid density and the critical current density. In order to study the temperature-dependent curves of the superfluid density and the critical current density, we applied an extended d-wave model to cuprate superconductors.

First, we examine the variation of the d-wave gap magnitude around the Fermi surface for the following cases: the extended d-wave gap with $B = 0.88$ for underdoped ($T_c = 80$ K) $Bi_2Sr_2CaCu_2O_{8+\delta}$ (Bi2212) [25]; $B = 1$ for overdoped Bi-2212 ($T_c = 80$ K) [25]; $B = 0.78$ for optimally doped ($T_c = 35$ K) $(Bi,Pb)_2(Sr,La)_2CuO_{6+\delta}$ (Bi-2201) [8]; and $B = 1.43$ for optimally doped ($T_c = 26$ K) electron-doped cuprate $Pr_{0.89}LaCe_{0.11}CuO_4$ (PLCCO) [16], respectively. Plots of the angular parts $g(\varphi)$ of the superconducting energy gaps for these cases are presented in Fig. 1a. The variation of gap's magnitudes for the same compounds is shown in Fig. 1b. Note an unusual value for B in the case of PLCCO that exceeds 1 and, as we show below, results in a quite different gap topology and resulting superfluid density as a function of temperature. Figure 1c also shows the angular part of the anisotropic s-wave function with two- and four-fold symmetry plotted on the polar graph as a dashed line ($A = 0.30$) and a solid line ($A = 0.25$), respectively.

Figure 2 shows the superconducting energy gap Δ of the above compounds as a function of normalized temperature (T/T_c) for the isotropic and the anisotropic s-wave, nodal d-wave, and the extended d-wave symmetries obtained from numerical solutions of the self-consistent gap equations. Taking a model d-wave gap, $\Delta(T,\varphi) = \Delta_0(T)[B\cos(2\varphi) + (1-B)\cos(6\varphi)]$, we have found that the temperature evolution of the extended d-wave gaps, shown in Fig. 2 are very similar to the isotropic gap but with a larger zero temperature gap of $\Delta(0) = 2.14k_BT_c$. Further, one can calculate the same for the case of the anisotropic s-wave gap, e.g. $\Delta(T,\varphi) = \Delta_0(T)[1 + A\cos(4\varphi)]$. This model gap has four-fold oscillations, similar to the two-fold of the nodal d-wave case, but is finite valued for all φ, while the parameter A describes the degree of anisotropy. If one takes $A = 0.292$, the maximum value of the anisotropic s-wave gap at $T \simeq 0$ K is $1.67k_BT_c$, The temperature dependence of the anisotropic s-wave type Δ shows very similar behaviour to the other cases, and lies between those graphics, corresponding to the isotropic s- and d-wave scenarios.

Further, the primary result is the temperature dependence of the superfluid density, calculated with the extended d-wave gap and the anisotropic s-wave gap in the form of Eqs. (2) and (4), respectively, as if all of this contributed to superconductivity. These dependencies are presented in Fig. 3 from which one can see that the superfluid density dependencies for the s- and d-wave cases are differ significantly. While this may in principle exist, this behavior is unlikely and implies that the spectral gap measured by ARPES in cuprate superconductors is a combination of a nodal d-wave ($B = 1$) superconducting gap and a pseudogap that does not contribute to condensation. However, the pseudogap affects the spectral density of quasiparticles, and this must be taken into account [15–19] when calculating the superfluid density. To reliably estimate the density of a superfluid density, accurate measurements of the temperature-dependent penetration depth as well as its value at zero temperature are required.

Now, let us compare our results of calculation of the superfluid density with experimental data in single layer tetragonal compound $Tl_2Ba_2CuO_{6+\delta}$ (Tl-2201) at almost optimally doping ($T_c = 78$ K) [26], in 15% Y-doped Bi-2212 (i.e., $Bi_{2.1}Sr_{1.9}Ca_{0.85}Y_{0.15}Cu_2O_{8+\delta}$) at

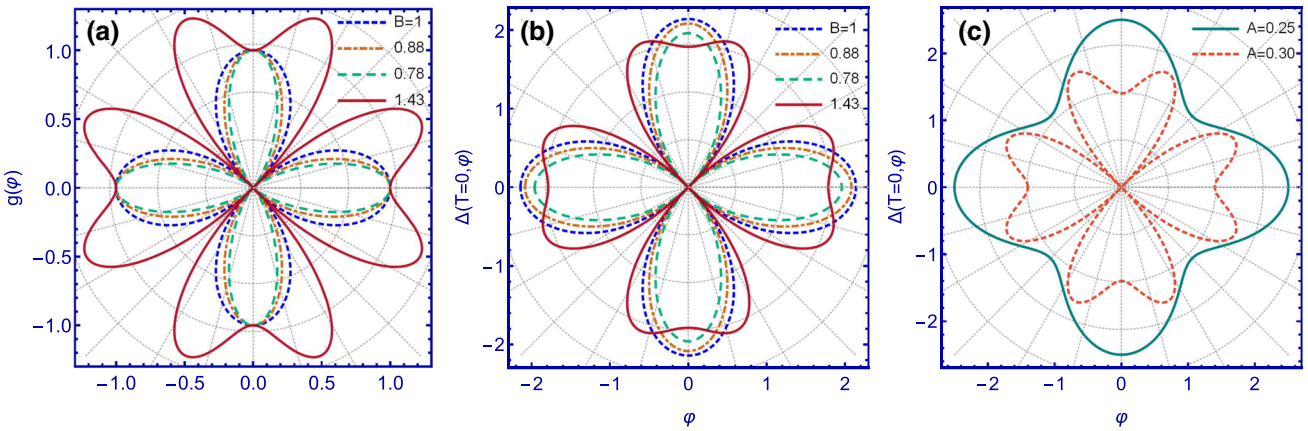

Fig. 1 **a** Angular part of the superconducting energy gap of underdoped Bi-2212 ($B = 0.88$), overdoped Bi-2212 ($B = 1$), optimally doped Bi-2201 ($B = 0.78$) and PLCCO ($B = 1.43$) cuprates. **b** Variation of the d-wave gap magnitudes of underdoped Bi-2212 ($B = 0.88$), overdoped Bi-2212 ($B = 1$), optimally doped Bi-2201 ($B = 0.78$) and PLCCO ($B = 1.43$) cuprates around the Fermi surface for each case. **c** Angular part of the anisotropic s-wave gap function is calculated using Eqs. (3) and (4) with two values of the anisotropy parameters

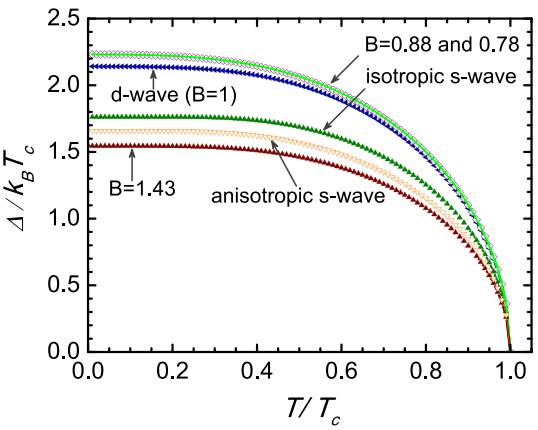

Fig. 2 Superconducting energy gap as a function of normalized temperature (T/T_c) for isotropic and anisotropic s-wave, nodal d-wave, as well as the extended d-wave symmetries obtained from numerical solutions of the self-consistent gap equations

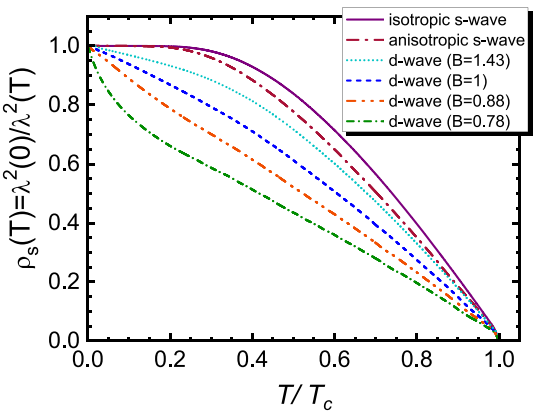

Fig. 3 The temperature dependence of the superfluid density calculated for isotropic and anisotropic s-wave, nodal d-wave (for $B = 1.0$), as well as three different non-monotonic d-wave gaps (for $B = 1.43$, 0.88, and 0.78), respectively

optimal doping, $\delta = 0.16$ (maximum $T_c = 90$ K) [27], and in pure Bi-2212 ($T_c = 93$ K) [28], respectively. Figure 4 shows the results of the d-wave calculations (solid lines, Eq. (20)). Symbols show the experimental data. To calculate the temperature dependence of the superfluid density, the superconducting gap parameter is obtained from the numerical solution of the self-consistent gap Eq. (21) with extended d-wave symmetry. Thus, for optimally doped Tl-2201, we take the value of parameter B equal to 0.9; $B = 0.88$ for 15% Y-doped Bi-2212; and $B = 1.0$ for pure Bi-2212, respectively. A characteristic feature of this theory is linear behavior of ρ_s at low temperatures. Here, the coincidence of calculations and experimental data can be considered as proof of d-wave pairing.

In Fig. 5, we compare our calculated ρ_s as a function of temperature with recent experimental AC susceptibility data given by Khasanov et al. [6] for electron-doped cuprate superconductor $Sr_{0.9}La_{0.1}CuO_2$. One feature of $\rho_s(T)$ in Fig. 5 is that the symmetry of the gap in electron-doped cuprates changes from a pure d-wave to an extended d-wave. The reason for this change is that the superfluid density in the superconducting state is especially sensitive to changes in anisotropy (i.e., to changes in parameter B) (see Ref. [25]). Furthermore, it is very important to note that at low temperatures $\rho_s(T)$ linear depends on the temperature.

For $B \geq 1$, the superfluid density exhibits normal convex behavior, while for $B < 1$, the behavior is concave. As proof of this, for electron-doped cuprates, our results show that the behavior differs significantly from that of hole-doped analogs, and the non-monotonic gap creates a superfluid density with $B = 1.43$, which indicates a significant contribution from the second harmonic of the $d_{x^2-y^2}$ order param-

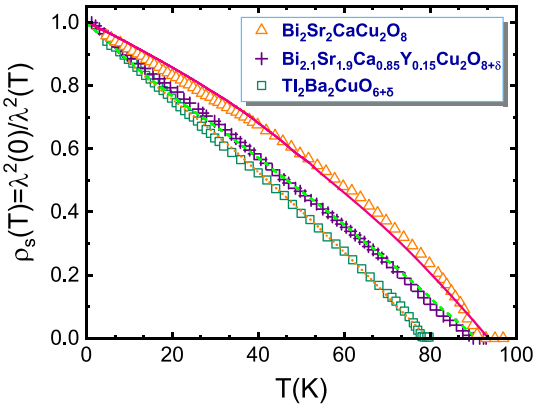

Fig. 4 The superfluid density ($\rho_s \propto \lambda^{-2}$) plotted as a function of temperature. Symbols: experimental data in single layer tetragonal compound $Tl_2Ba_2CuO_{6+\delta}$ (T_c = 78 K) [26], experimental AC susceptibility data in $Bi_{2.1}Sr_{1.9}Ca_{0.85}Y_{0.15}Cu_2O_{8+\delta}$ at optimal doping, $\delta = 0.16$ (maximum $T_c = 90$ K) [27] and in $Bi_2Sr_2CaCu_2O_8$ ($T_c = 93$ K) [28]. Solid lines show the results of the d-wave calculations

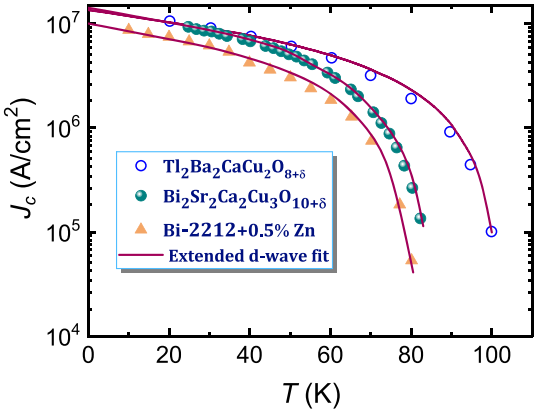

Fig. 6 Comparison of the theoretical results for $J_s(T)$ calculated with the extended d-wave gap (solid line) with the corresponding experimental data obtained from [29] (open circles) for $Tl_2Ba_2CaCu_3O_{8+\delta}$, from [30] (solid circles) for $Bi_2Sr_2CaCu_2O_{10+\delta}$ and from [31] (solid triangles) for a 0.5% Zn-doped Bi-2212

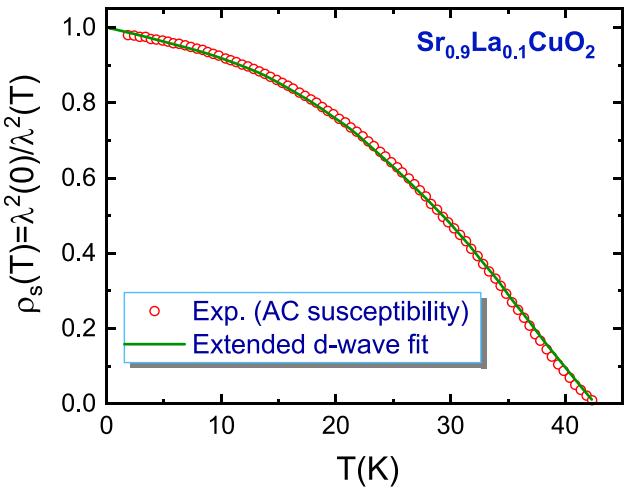

Fig. 5 Comparison of our calculated results for $\rho_s(T)$ (solid line) with experimental AC susceptibility data (open circles) reported by Khasanov et al. [6] for electron-doped cuprate superconductor $Sr_{0.9}La_{0.1}CuO_2$

eter. We have demonstrated that the non-monotonic gap function, Eq. (2), should lead to an unusual sub-linear temperature dependence of ρ_s. It is quite possible that such an unusual gap structure is the result of the interference of a superconducting gap and a pseudogap. In this case, the superfluid density is determined only by the superconducting gap, and measurements of the penetration depth will be very useful for elucidating physics.

Let us now consider the critical current density J_c, which is one of the main characteristics of high-T_c superconductors. It is known that the critical current density is strongly temperature dependent. In this work, for comparison, we used expression (22) for the critical current density in zero magnetic field ($H = 0$). The critical current density $J_c(T)$ is calculated as a function of temperature and compared with the experimental data, as shown in Fig. 6. To perform these fits, we used an extended d-wave gap with $B = 0.88$. In Fig. 6 shows the experimental data for the epitaxial $Tl_2Ba_2CaCu_3O_8$ thin films, obtained by Holstein et. al. [29] (open circles), for the epitaxial $Bi_2Sr_2CaCu_2O_{10+\delta}$ thin films, obtained by Hänisch et. al. [30] (solid circles), and for a 0.5% Zn-doped Bi-2212 thin film, obtained by Wagner et al. [31] (solid triangles). In the numerical calculations of $J_c(T)$, we used the following parameters in order to obtain the best fit: the superfluid density at a temperature of almost zero Kelvin, $\rho_s(0)$ is equal to 0.73×10^{19} cm^{-3}, $m_c = 1.8m_e$, (where m_e is the mass of a free electron) and the value of $T_c = 100$ K for $Tl_2Ba_2CaCu_3O_8$; $\rho_s(0) = 0.67 \times 10^{19}$ cm^{-3}, $m_c = 1.4m_e$, and $T_c = 86$ K for $Bi_2Sr_2CaCu_2O_{10+\delta}$; $\rho_s(0) = 0.8 \times 10^{19}$ cm^{-3}, $m_c = 2.2m_e$ and $T_c = 80$ K for Bi-2212+0.5% Zn, respectively.

Figure 7 shows $J_c(T)$ curves for the mixed rare earth (Nd,Eu,Gd)$Ba_2Cu_3O_7$ thin films in the zero magnetic field. Experimental $J_c(T)$ data obtained by Cai et. al. [32] for the mixed rare earth thin films of (Nd,Eu,Gd)$Ba_2Cu_3O_{7-\delta}$ (NEG123) and $GdBa_2Cu_3O_{7-\delta}$ (Gd123), and the respective theoretical fitting curves calculated with the extended d-wave gap.

We obtained reasonable fits to the experimental data by taking appropriate sets of parameters: $B = 1.0$, $\rho_s(0) = 2.3 \times 10^{19}$ cm^{-3}, $m_c = 1.8m_e$, and $T_c = 88$ K for NEG123 and $B = 0.9$, $\rho_s(0) = 1.6 \times 10^{19}$ cm^{-3}, $m_c = 2m_e$, and $T_c = 86$ K for Gd123, respectively. The extrapolated values of J_c at $T \simeq 0$ K are $J_c(T \simeq 0) \gtrsim 29.94\,\mathrm{MA/cm^2}$ and $J_c(T \simeq 0) \gtrsim 23.29\,\mathrm{MA/cm^2}$ (for the compounds NEG123 and Gd123), respectively.

Finally, our fitting results within the extended d-wave gap (with $B = 0.92$) to the experimental $J_c(T)$ data are shown in Fig. 8 for d-wave superconducting nanowires $YBa_2Cu_3O_{7-\delta}$ (YBCO). Experimental data for YBCO

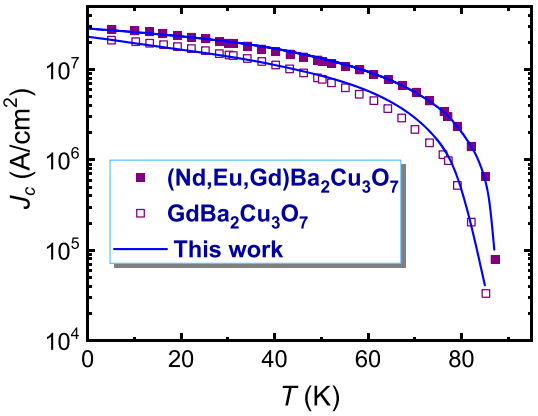

Fig. 7 Experimental $J_c(T)$ data obtained by Cai et. al. [32] (all symbols) for the mixed rare earth thin films of (Nd,Eu,Gd)$Ba_2Cu_3O_{7-\delta}$ (filled squares) and $GdBa_2Cu_3O_{7-\delta}$ (open squares), and the respective theoretical fitting curves calculated with the extended d-wave gap (solid line). $J_c(T)$ in (Nd,Eu,Gd)$Ba_2Cu_3O_{7-\delta}$ is improved in comparison with in $GdBa_2Cu_3O_{7-\delta}$

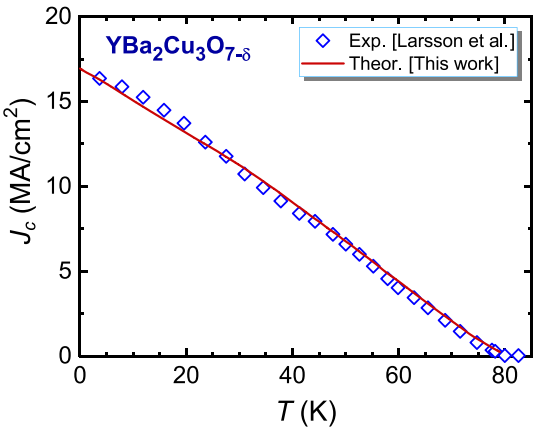

Fig. 8 Experimental $J_c(T)$ data obtained from [33] (open symbols) for d-wave superconducting nanowires $YBa_2Cu_3O_{7-\delta}$ (with $aa = 136$ nm and $bb = 50$ nm) and the corresponding theoretical fit curve calculated with the extended d-wave gap (solid line)

obtained by Larsson et al. [33]. We use the following sets of intrinsic materials parameters in order to obtain the best fits: $\rho_s(0) = 1.55 \times 10^{19}$ cm^{-3}, $m_c = 2.3m_e$, and $T_c = 80$ K, respectively. The extrapolated value of J_c at $T \simeq 0$ K is $J_c(T \simeq 0) \gtrsim 16.94\,\mathrm{MA/cm^2}$.

It is important to emphasize that although the temperature dependence of some quantities can give an idea of the gap structure in a cuprate superconductor, it is important to take into account the role of impurity scattering in these processes. In particular, impurity scattering caused by chemical impurities or physical disorder can change the expected temperature dependence of the magnetic penetration depth due to the effect of scattering on the low energy density of states relative to the Fermi level. For clean d-wave symmetry the change in the penetration depth as a function of temperature is linear in temperature ($\Delta\lambda(T) \propto T$), whereas a quadratic temperature dependence ($\Delta\lambda(T) \propto T^2$) is expected if the nodes are filled by impurity states. It is well known that the so-called "dirty d-wave" theory of cuprate superconductivity is an extension of the original field-theoretical formulation of disordered superconductors proposed by Abrikosov and Gor'kov [34,35]. According to Abrikosov–Gor'kov theory [34,35], the transition between gap and gapless regimes was regulated by the concentration of pair-breaking impurities and the properties of such superconducting systems were studied within the mean-field approximation. This theory was applied for the first time to unconventional superconductors by Gor'kov and Kalugin [36,37] and by Ueda and Rice [38], and was also extended to arbitrary impurity phase shifts by Hirschfeld et al. [39] and Schmitt-Rink et al. [40]. The influence of impurities on the superfluid density of heavy-fermion superconductors was considered within the framework of the same formalism by Gross et al. [41], and applied to d-wave superconductors by Prohammer and Carbotte [42] and Hirschfeld and Goldenfeld [43]. The latter work focused on strong scattering in an attempt to explain the penetration depth experiments of Zn-substituted YBCO by Bonn and co-workers who proved the existence of d-wave superconductivity in cuprates [44,45].

Over the past few years, Broun and collaborators [46–48] have calculated superfluid density, optical conductivity, residual heat capacity, Volovik effect, and thermal conductivity within the framework of dirty d-wave theory, and also compared with experiments on the overdoped $La_{2-x}Sr_xCuO_4$ (LSCO). They showed that the dirty d-wave theory agrees well with experimental data in the overdoped region. In this regard, they argue that the measurements on both the superfluid density and the optical conductivity of LSCO films can be understood almost entirely within a dirty d-wave scenario based on weak-coupling BCS theory [46,47]. Specifically, the effects of impurity scattering were treated within the self-consistent t-matrix approximation (SCTMA), in weak-coupling BCS theory. According to the SCTMA, impurities are treated as isotropic point scatters and are characterized by a scattering strength, c, which is the cotangent of the s-wave scattering phase shift. SCTMA calculations are usually performed in the case of weak scattering, where $c >> 1$ (Born limit) and in the case of strong scattering, where $c = 0$ (unitary limit). Both kinds of scattering will cause pair-breaking and lead to $\Delta\lambda/T^2$ below some crossover temperature T^*, and a linear behaviour above this temperature. The key parameter in the SCTMA analysis is $\Gamma_N(0)$, the zero-temperature normal state scattering rate. Disorder leads to a closing of the energy gap at a reduced T_c, the reduction being set by the Abrikosov-Gorkov formula [34,35]. It is important to note that T_c only depends on $\Gamma_N = T_{c0}$, while the form of $\rho_s(T)$ is heavily influenced by the impurity phase shift. Lee-Hone et al. [46] found to reproduce both the magnitude of the superfluid density and its (predominantly linear) dependence on temperature, provided that the vast majority of impurity scatters were in the Born limit. It

should be noted that the results of calculations in the framework of the BCS dirty d-wave theory performed by Broun and collaborators seem to explain many of the qualitative and quantitative features of the superfluid density and optical conductivity of overdoped LSCO [46,47].

Due to particular purpose in the present work, the effect of impurity scattering on the superfluid density, as well as the mechanism of nanoscale electronic disorder in cuprate superconductors, has not been considered. We want to emphasize that a series of experimental [7,8] and theoretical works [11] indicate that the angular dependence of the gap in electron-doped HTSCs significantly differs from the simple functional form $\Delta = \Delta_0 \cos(2\varphi)$ and has the nonmonotonic functional form of the $d_{x^2-y^2}$-wave superconducting gap (with a maximum gap between nodal and anti-nodal points on the Fermi surface). Although the temperature dependence of the anisotropic d-wave contribution to the superfluid density is very close to the quadratic (T^2) dependence (which is often observed in electron-doped HTSs) in general, the T^2 behavior is attributed to a dirty d-wave scenario and is explained by impurity scattering of the carriers. However, it is difficult to explain how an order parameter that changes sign persists in the dirty limit, since any scattering centers would act as pair breakers [49]. Thus, the results presented in this work should be attributed to pure superconductors. Consideration of superfluid density for a dirty d-wave superconductor is done in Ref. [46].

5 Conclusions

In summary, we considered the question of the influence of pairing symmetry on the superconducting gap $\Delta(T)$ and the superfluid density $\rho_s(T)$, as well as on the critical current density $J_c(T)$ in some superconducting cuprates. In this context, to calculate the superfluid density as well as $J_c(T)$ the temperature dependence of the gap magnitude was determined from the self-consistent gap equation of the gap depends on the pairing symmetry. Based on this, we used generalized BCS-like expressions to calculate $\Delta(T)$ with the pairing symmetry, as well as taking into account the extended d-wave gap with the next angular harmonic. We used these expressions for non-linear fitting of experimental ρ_s and J_c data sets for d-wave superconductors in thin films and nanowires.

Finally, we conclude that the above quantitative analysis of $\rho_s(T)$ data shows that the Chandrasekhar and Einzel approach with an extended d-wave gap describes consistently both concave and T-linear behavior of ρ_s at low temperatures, as well as non-linear behavior at high temperatures. In this respect, theoretical calculations are in excellent agreement with experimental data and show that the superfluid density and the critical current density of cuprates are well described by an extended d-wave gap with higher angular harmonics.

Data Availability Statement The manuscript has associated data in a data repository. [Authors' comment: All data included in this manuscript are available upon request by contacting the corresponding author.]

References

1. N.E. Bickers, D.J. Scalapino, Ann. Phys. **193**, 206–251 (1989)
2. J. Annett, N. Goldenfeld, S.R. Renn, Phys. Rev. B **43**, 2778–82 (1991)
3. P. Monthoux, A.V. Balatsky, D. Pines, Phys. Rev. Lett. **67**, 3448–51 (1991)
4. Z.X. Shen et al., Phys. Rev. Lett. **70**, 1553–1556 (1993)
5. H. Ding et al., Phys. Rev. Lett. **54**, 9678–9681 (1996)
6. R. Khasanov, A. Shengelaya, R. Brütsch, H. Keller, Condens. Matter **5**, 50 (2020)
7. G. Blumberg, A. Koitzsch, A. Gozar, B.S. Dennis, C.A. Kendziora, Phys. Rev. Lett. **88**, 107002 (2002)
8. H. Matsui, K. Terashima, T. Sato, T. Takahashi, M. Fujita, K. Yamada, Phys. Rev. Lett. **95**, 017003 (2005)
9. L. Shan et al., Phys. Rev. B **72**, 144506 (2005)
10. K. Okazaki et al., Phys. Rev. Lett. **109**, 237011 (2012)
11. I. Eremin, E. Tsoncheva, A.V. Chubukov, Phys. Rev. B **77**, 024508 (2008)
12. R. Prozorov, R.W. Giannetta, Supercond. Sci. Technol. **19**, R41–67 (2006)
13. R. Prozorov, V.G. Kogan, Rep. Prog. Phys. **74**, 124505 (2011)
14. A. Damascelli, Z. Hussain, Z.-X. Shen, Rev. Mod. Phys. **75**, 473 (2003)
15. W.S. Lee, I.M. Vishik, K. Tanaka, D.H. Lu, T. Sasagawa, N. Nagaosa, T.P. Devereaux, Z. Hussain, Z.X. Shen, Nature **458**, 81 (2007)
16. T. Kondo, T. Takeuchi, A. Kaminski, S. Tsuda, S. Shin, Phys. Rev. Lett. **98**, 267004 (2007)
17. T. Kondo, Y. Hamaya, A.D. Palczewski, T. Takeuchi, J.S. Wen, Z.J. Xu, G. Gu, J. Schmalian, A. Kaminski, Nat. Phys. **7**, 21–25 (2011)
18. I.M. Vishik et al., PNAS **109**, 18332–18337 (2012)
19. I.M. Vishik, Rep. Prog. Phys. **81**, 062501 (2018)
20. Ø. Fischer, M. Kugler, I. Maggio-Aprile, C. Berthod, C. Renner, Rev. Mod. Phys. **79**, 353 (2007)
21. K.K. Gomes, A. Pasupathy, A. Pushp, S. Ono, Y. Ando, A. Yazdani, Nature **447**, 569 (2007)
22. A.C. Fang, L. Capriotti, D.J. Scalapino, S.A. Kivelson, N. Kaneko, M. Greven, A. Kapitulnik, Phys. Rev. Lett. **96**, 017007 (2006)
23. K. McElroy, D.-H. Lee, J.E. Hoffman, K.M. Lang, E.W. Hudson, H. Eisaki, S. Uchida, J. Lee, J.C. Davis, Phys. Rev. Lett. **94**, 197005 (2005)
24. B.S. Chandrasekhar, D. Einzel, Annalen der Physik **505**, 535546 (1993)
25. J. Mesot, M.R. Norman, H. Ding, M. Randeria, J.C. Campuzano, A. Paramekanti, H.M. Fretwell, A. Kaminski, T. Takeuchi, T. Yokoya, T. Sato, T. Takahashi, T. Mochiku, K. Kadowaki, Phys. Rev. Lett. **83**, 840 (1999)

26. D.M. Broun, D.C. Morgan, R.J. Ormeno, S.F. Lee, A.W. Tyler, A.P. Mackenzie, J.R. Waldram, Phys. Rev. B **56**, R11443(R) (1997)
27. W. Anukool, S. Barakat, C. Panagopoulos, J.R. Cooper, Phys. Rev. B **80**, 024516 (2009)
28. S.-F. Lee, D.C. Morgan, R.J. Ormeno, D.M. Broun, R.A. Doyle, J.R. Waldram, K. Kadowaki, Phys. Rev. Lett. **77**, 735–8 (1996)
29. W.L. Holstein, C. Wilker, D.B. Laubacher, D.W. Face, P. Pang, M.S. Warrington, C.F. Carter, L.A. Parisi, J. Appl. Phys. **74**, 1426–1430 (1993)
30. J. Hänisch, A. Attenberger, B. Holzapfel, L. Schultz, Phys. Rev. B **65**, 052507 (2002)
31. P. Wagner, F. Hillmer, U. Frey, H. Adrian, Phys. Rev. B **49**, 13184 (1994)
32. C. Cai, B. Holzapfel, J. Hänisch, L. Fernández, L. Schultz, Appl. Phys. Lett. **84**, 377 (2004)
33. P. Larsson, B. Nilsson, Z.G. Ivanov, J. Vac. Sci. Technol B Microelectron Nanometer Struct **18**, 25 (2000)
34. A.A. Abrikosov, L.P. Gor'kov, Zh Eksp, Teor. Fiz. **39**, 1781 (1960)
35. A.A. Abrikosov, L.P. Gor'kov, Sov. Phys. JETP **12**, 1243 (1961)
36. L.P. Gor'kov, P.A. Kalugin, Pis'ma. Zh. Eksp. Teor. Fiz. **41**, 208 (1985)
37. L.P. Gor'kov, P.A. Kalugin, JETP Lett. **41**, 253 (1985)
38. K. Ueda, M. Rice, in Theory of Heavy Fermions and Valence Fluctuations, edited by T. Kasuya and T. Saso (Springer, Berlin, 1985)
39. P. Hirschfeld, D. Vollhardt, P. Wölfle, Solid State Commun. **59**, 111 (1986)
40. S. Schmitt-Rink, K. Miyake, C.M. Varma, Phys. Rev. Lett. **57**, 2575 (1986)
41. F. Gross, B.S. Chandrasekhar, D. Einzel, K. Andres, P.J. Hirschfeld, H.R. Ott, J. Beuers, Z. Fisk, J.L. Smith, Z. Phys. B **64**, 175 (1986)
42. M. Prohammer, J.P. Carbotte, Phys. Rev. B **43**, 5370 (1991)
43. P.J. Hirschfeld, N. Goldenfeld, Phys. Rev. B **48**, 4219 (1993)
44. W.N. Hardy, D.A. Bonn, D.C. Morgan, R. Liang, K. Zhang, Phys. Rev. Lett. **70**, 3999 (1993)
45. D. Achkir, M. Poirier, D.A. Bonn, R. Liang, W.N. Hardy, Phys. Rev. B **48**, 13184 (1993)
46. N.R. Lee-Hone, J.S. Dodge, D.M. Broun, Phys. Rev. B **96**, 024501 (2017)
47. N.R. Lee-Hone, V. Mishra, D.M. Broun, P.J. Hirschfeld, Phys. Rev. B **98**, 054506 (2018)
48. N.R. Lee-Hone, H.U. Özdemir, V. Mishra, D.M. Broun, P.J. Hirschfeld, Phys. Rev. Res. **2**, 013228 (2020)
49. A.J. Millis, S. Sachdev, C.M. Varma, Phys. Rev. B **37**, 4975–4986 (1988)